Received: 29 September 2023 | Revised: 20 February 2024 | Accepted: 17 March 2024

DOI: 10.1002/cnm.3817

APPLIED RESEARCH

WILEY

Semi-automatic algorithm to build finite element numerical models of the human hearing system from Micro-CT data

L. Caminos | **G. Chaves** | **J. Garcia-Manrique** | **A. Gonzalez-Herrera**

Departament of Civil, Materials and Manufacturing Engineering University of Malaga, Málaga, Spain

Correspondence
L. Caminos, Departament of Civil, Materials and Manufacturing Engineering, University of Malaga Escuela de Ingenierías Industriales, C/ Doctor Ortiz Ramos, s/n. Campus de Teatinos, E-29071, Málaga, Spain.
Email: lfcaminos@uma.es

Funding information
European Regional Development Fund, Grant/Award Number: UMA18-FEDERJA-214; Universidad de Málaga/CBUA

Abstract

Finite Element modeling has been an extended methodology to build numerical model to simulate the behavior of the hearing system. Due to the complexity of the system and the difficulties to reduce the uncertainties of the geometric data, they result in computationally expensive models, sometimes generic, representative of average geometries. It makes it difficult to validate the model with direct experimental data from the same specimen or to establish a patient-oriented modeling strategy. In the present paper, a first attempt to automatize the process of model building is made. The source information is geometrical information obtained from CT of the different elements that compose the system. Importing that data, we have designed the complete procedure to build a model including tympanic membrane, ossicular chain and cavities. The methodology includes the proper coupling of all the elements and the generation of the corresponding finite element model. The whole automatic procedure is not complete, as we need to make some human-assisted decisions; however, the model development time is reduced from 4 weeks to approximately 3 days. The goal of the modeling algorithm is to build a Finite Element Model with a limited computational cost. Several tasks as contour identification or model decimation are designed and integrated in order to follow a semi-automated process that allows generating a patient-oriented model.

KEYWORDS

finite element model, human hearing, middle ear

1 | INTRODUCTION

In recent years, numerical simulations of specific models of different pathologies in patients have been developed in various medical specialties in order to understand them more thoroughly and find more effective treatments.[1–5] This

Abbreviations: AC, auditory canal; AS, auditory system; CT, computed-tomography; EC, ear canal; FEM, finite element method; KP, key point; ME, middle ear; MF, manubrial fold; OC, ossicular chain; TC, tympanic cavity; TM, tympanic membrane.

requires, in most cases, the use of images to generate the models. The complexity of biological forms and materials makes the construction of these models a laborious task with a high investment of time. Therefore, it is necessary to generate methodologies that automate the process of building specific geometries and models for each patient.

The Finite Element method is commonly used to build numerical models to simulate the human hearing system behavior, which has allowed important advances in the understanding of this complex system[6–15]; the geometric models, as well as materials properties, are fundamental for achieving good results. Although there have been significant advances in this field, it is necessary to transfer this knowledge to methodologies that make it possible to generate models oriented to each specific patient.

Micro-CT images are used to build the geometry of the components of the human ear, as they offer a high level of detail.[16–19] They are processed using specialized software to convert into compatible formats with finite element programs; sometimes, they are smoothed to avoid inappropriate aspect ratios before the meshing process, and in other cases, their quality is reduced to save computational costs. Finally, the geometry obtained is coupled and spatially positioned using specific reference systems.

Recently, high-speed digital holographic (HDH) is already used to obtain measurements of TM movements induced by acoustic impulses that allow to obtain external geometric of TM and accurate information about its dynamic properties.[20,21]

This paper aims to show the development and application of an algorithm that automates most of the finite element modeling process of the human hearing system: EC, TM, OC, and TC. The final goal is to build a Finite Element Model with an improved computational cost even though operations, such as contour identification, model decimation, element identification, joints implementations or contour conditions are included in the algorithm following a semi-automated process.

Section 2 describes the algorithm and its implementation to build the model. Section 3 describes the building process of the different geometries and their subsequent positioning in the final FEM. Also, the results of simulations, applying modal and harmonic analysis, are compared with previous works to verify the accuracy of the model. Finally, the main conclusions are highlighted in Section 4.

2 | MATERIALS AND METHODS

A brief description of the general procedure is made in this section. First a general overview of the algorithm will be made and then the general issues for Finite Element modeling will be stated.

2.1 | Algorithm: General issues

The structure of this algorithm (Figure 1) is the main purpose of the present work. Not all the steps have been completely automated, but the complete process has been already designed. An outline of the procedure is described now and will be detailed in the following sections.

It starts with a geometric input data and two basic steps are needed before obtaining the FE model: (a) a decimation process and (b) coupling process. After those key processes, the model is meshed, and boundary conditions are applied.

Input data can be obtained from Micro-CTs of the hearing system. In the present work we have used the geometric data of ME taken from Laboratory of Biomedical Physics of University of Antwerp. The Micro-CT reconstruction data were segmented using a combination of manual and automatic tools from the AMIRA® software. The final geometry consists of a surface formed by contiguous triangles, obtained from the triangulation algorithm of the program itself (STL file). Details of sample preparation and use of the software are described in.[19] For the EC and TC, we will use a simplified geometries previously used by our research group in other works.[22–25]

Due to the high levels of precision that Micro-CT provides currently, the geometric data of ME, is detailed in excess for the purpose of FE modeling and computation. It increases the computational cost without a clear advantage on the quality of the results. So, a decimation process is necessary as a first step. It is made on the OC and TM using Matlab and ANSYS software. The description of this process is shown in Sections 3.1 and 3.2. In this work, the EC and the TC are already simplified, so this step is avoided, but in a general case, a process similar to that described for the OC and MT would be followed.

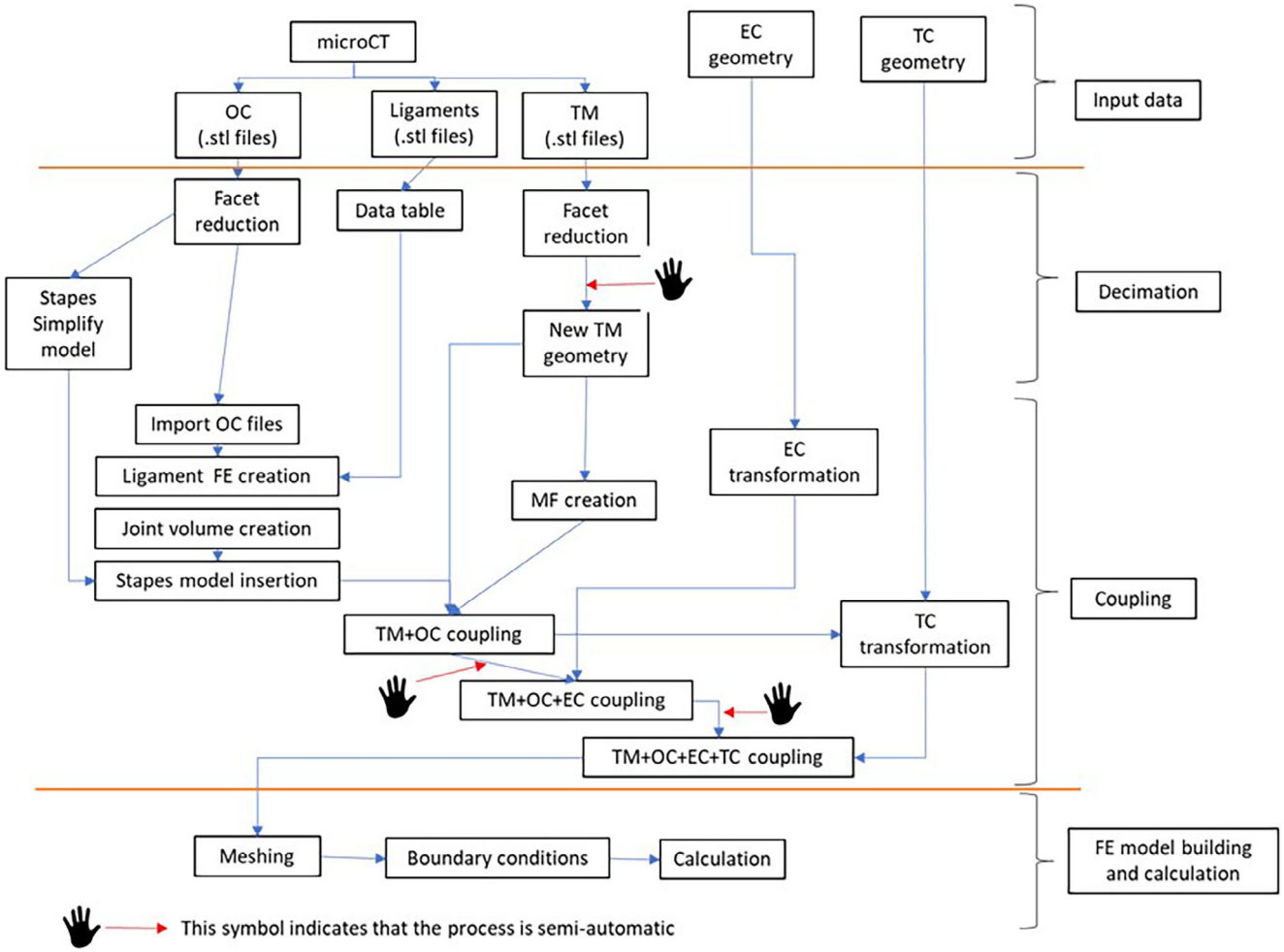

FIGURE 1 Algorithm scheme.

Once we have the new decimated geometries in the form of CAD files or data table, we proceed to the coupling of the different component. Even when the original data comes from the same specimen, coupling is not an easy step. This is the point where automation of the decision-making is more complex. We need to couple geometries with different characteristic, adding ligament and joint, and at the same time ensuring that the meshing step can be made in an efficient way. This process is described in Sections 3.1–3.3.

2.2 | FEM: General issues

A summary of the main modeling methodology developed in our work is presented in this section. It has been developed from precedent works.[6–8,10–12,26–28] In some case the own methodology has been object of our study.[22,23,25–29] Key aspects have been studied and adjusted to achieve a model representative of the auditory system. Linear elastic material behavior was assumed in this study. This hypothesis is based on the commonly accepted fact of linearity of the middle ear with sound pressures below 90 dB. Muscles contraction mechanisms (which cause non-linearity) are not actives. On the other hand non-linearity may occur in the inner ear as amplification effect of active mechanisms that are not considered in this study.

The finite element model of all the system was generated using ANSYS. The air in the auditory canal is meshed with acoustic elements (FLUID30) which behave according to the acoustic wave equation assuming a compressible and inviscid fluid with uniform mean density and pressure. The total volume of air is 1342 mm^3, the speed of sound is 343 m/s and density 1.21 kg/m^3. The acoustic absorption coefficient for the tympanic membrane and the canal wall are 0.007 and 0.02 respectively (from Gan et al.[7]).

The TM was modeled with solid elements (SOLID 185) assuming uniform thickness of 0.05 mm. For the OC, posterior incudal ligament, incudomalleolar and incudostapedial joints, solid (SOLID185) elements are used. The ligaments and tendon support of the malleus are modeled with beam (BEAM182) elements.

The boundary conditions of the model include the suspensory ligaments and tendons of the OC, which are joined at one end with the nodes at the intersection of each bone and, at the other end, are fixed to simulate the union with the TC. The nodes of the outer edge of the MT too are fixed to simulate the connection with the TC. The cochlear load on stapedial footplate was modeled with a viscoelastic equivalent system according to.[11] For this a COMBIN 14 element is used, the stiffness and damping are 60 N/m and .054 N/(m s) respectively.

The mechanical properties of the components of the model, were taken from the mean values commonly accepted in the literature and are shows in Table 1. Most of the information comes from calibration with numerical models.

These values and boundary conditions have been used in previous works to evaluate the dynamic behavior of the human middle and external ear. The simulation responses have been contrasted with experimental measurements from the literature. A sensitivity analysis is shown in (Figure 2).[25]

A mesh convergence study is made for the TM, as it is the most critical geometry.[30] The form factor (ratio between the element and the TM thickness) used is three. The FEM is meshed in an ordered manner, starting with both joints,

TABLE 1 Mechanical properties used in middle ear components for finite element model.

Component	Density $\times 10^3$ (Kg/m^3)	Young's modulus (N/m^2)	Poisson's ratio
TM	1.2[12]	3.2×10^7[10]	.3[11]
Manubrial fold	1.2[26]	10% of TM[26]	.49[26]
Malleus	1.9[27]	1.41×10^{28}	.3[11]
Incus	1.9[27]	1.41×10^{28}	.3[11]
Stapes	1.9[27]	1.41×10^{28}	.3[11]
Tensor tympanic tendon	2.5[6]	2.6×10^6[6]	.3[11]
Lateral mallear ligament	2.5[6]	6.7×10^4[6]	.3[11]
Anterior mallear ligament	2.5[6]	2.1×10^6[6]	.3[11]
Superior mallear ligament	2.5[6]	4.9×10^4[6]	.3[11]
Posterior incudal ligament	2.5[6]	6.5×10^6[7]	.3[11]
Stapedial tendon	2.5[6]	5.2×10^5[6]	.3[11]
Incudomalleolar joint	3.2[11]	1.41×10^{10}[11]	.3[11]
Incudostapedial joint	1.2[11]	6×10^5[8]	.3[11]

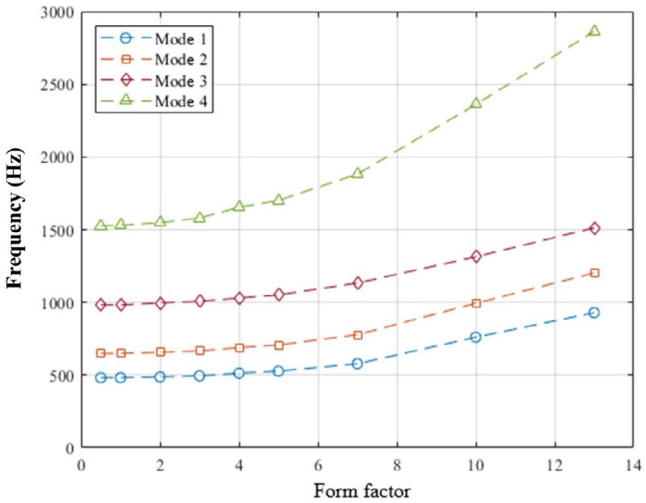

FIGURE 2 TM mesh convergence study.

following by malleus, incus and stapes, TM, and MF. For fluid simulations, EC and TC are meshed at the end. The completed geometry has fully restricted nodes at the ends of ligaments, and at the TM perimeter. A two-axis restriction is taken for the stapes footplate perimeter. The entire meshing process is automated using ANSYS taking into account the quality parameters of the mesh.

3 | RESULTS

In this section we will detail key aspects of three main tasks needed to build the model and how they have been automated.

3.1 | Ossicular system

Due to the stiffness of the bone relative to the soft tissues of the system, the FE model does not need a high number of elements to model the ossicles. However, its complex geometry makes difficult to reduce this unnecessary computational cost. So, CT ossicles information must be simplified.

This is done by decreasing external geometry facet number. A routine programmed in Matlab software is used for this task. Malleus, incus, stapes volumes have this treatment.

The STL files of the ossicles obtained from the Micro-CT scanner are processed using the Matlab program. With this software, a program was created capable of simplifying the faceting of the original files, making use of the characteristic programming of files with an STL extension and different Matlab tools, finally obtaining a considerable reduction in the number of faces.

The new STL files from Matlab are imported into ANSYS Mechanical APDL, for which the *SpaceClaim* software was used. In this, the import was configured to match the outgoing Matlab STL file, to which automated corrections were made with the software itself before saving them as Parasolid type files with an .x_t extension.

Results are shown in Figure 3.

Ligaments and tendons are modeled with a different strategy. They are modeled with beam elements. In this work the process is not automated, but it can easily be done. A data table is written to incorporate them to the model building process. Their geometries are a hybrid between CT and reference information.[9,17,31] The length is taken from the ends of unmodified CT data. Table 2 shows the referenced diameter of these components.

The incudomalleolar and incudostapedial joints are not imported geometries, they are created inside the space among the connecting ossicles. Simplified geometries (a disc and a sphere respectively) are build and intersected with the ossicles (Figure 4). So, the volumes created represent with enough accuracy the joints with a limited computational cost.

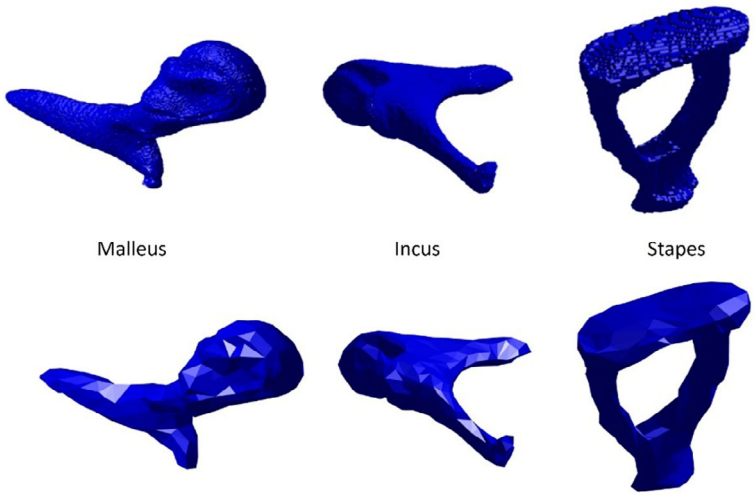

FIGURE 3 Ossicles: malleus, incus, and stapes. Top: facet original. Bottom: facet reduction.

TABLE 2 Diameters used in ligaments and tendons.

Component	Diameter (mm)
Tensor tympanic tendon	.80[17]
Lateral mallear ligament	.55[17]
Anterior mallear ligament	.90[17]
Superior mallear ligament	.25[17]
Posterior incudal ligament	.50[9]
Stapedial tendon	.40[31]

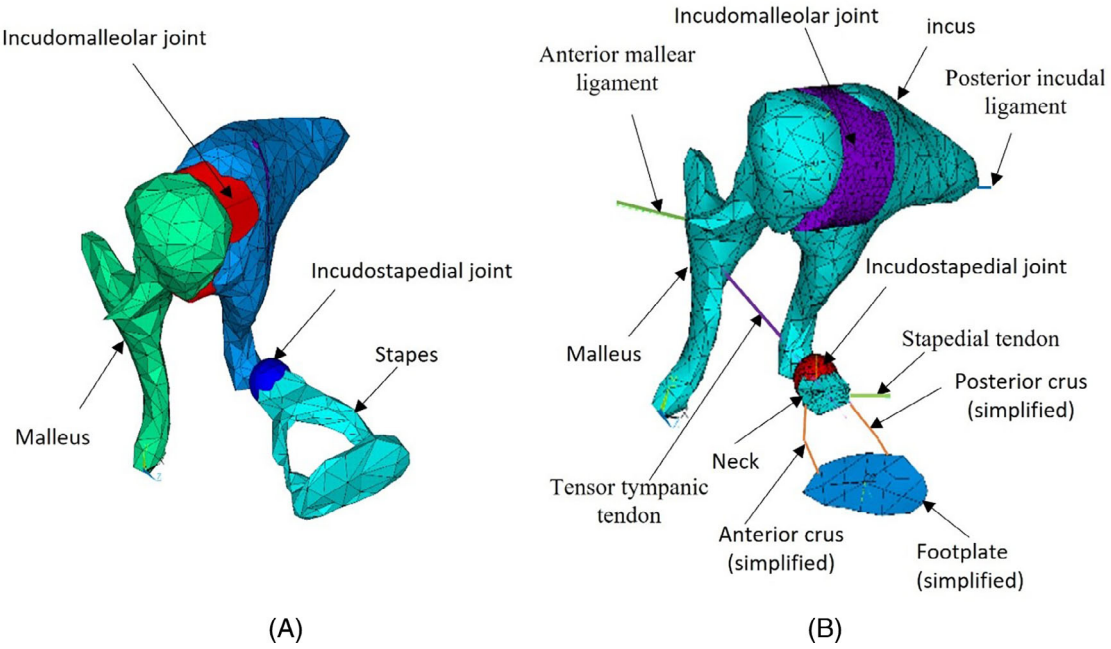

FIGURE 4 Ossicular chain model. (A) Original stapes. (B) Simplified stapes, ligaments, and tendons.

In this case, the stapes has followed an additional simplification. This step is not necessary, but it reduces the computational cost and has been evaluated. Due to its complex faceted geometry, when it is meshed, the number of elements used is unnecessarily high. A new footplate is done using the lines of the original perimeter and meshed with shell element. It results in a 2-D surface with a given thickness. The head remains unmodified. The stapes is cut off at the neck. Both cruses are simplified by a pair of lines following the curvature (Figure 4B). This step is not automatic.

The results obtained using this equivalent system agree with those obtained in previous simulations and experiments. Validation of this system can be reviewed in.[24]

3.2 | Membrane limit identification

The TM is one of the elements more difficult to identified on the CT[19] and consequently its geometrical model is difficult to use in a FE model when it must be meshed with solids elements. It has been completely redone after the facet reduction process (using Matlab). ANSYS software is used for this purpose (Figure 5). The TM algorithm use CT data points to search critical regions. These regions are divided in external perimeter, superior ring, manubrium area, intermediate area, and central area.

The external perimeter decimation starts by searching the maximum and minimum values in the main axes. The *Y*-axis is divided in a finite number of portions. The number of divisions is a parameter selected by the user. The algorithm does a loop to find the maximum and minimum value in *X* axis for every division of *Y* axis. The information of

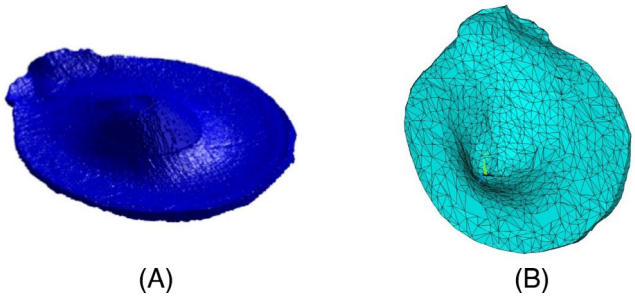

FIGURE 5 Tympanic membrane. (A) Geometry obtained from the CT. (B) FE model obtained from ANSYS.

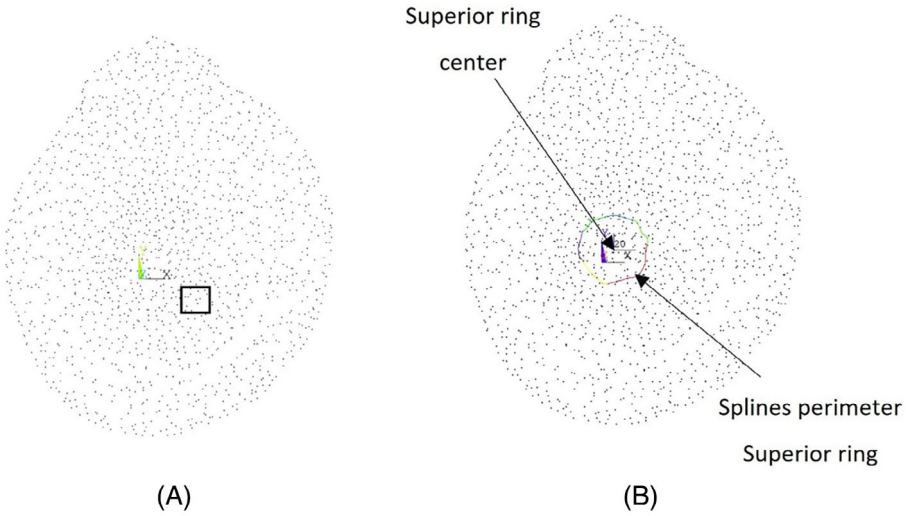

FIGURE 6 Data points of TM. (A) Point cloud obtained from the CT. (B) Point cloud new and splines perimeter superior ring.

those points is stored in an orderly manner in new points. A new point cloud is created. Axis *Z* values are standardized by using its medium value. A loop makes the splines that form the new perimeter. This process is completely automatic.

The superior ring study starts by searching its centre. This search is restricted at the *Z* axis, the user selects where introducing a factor. Once the range is known, the algorithm creates new key points (KP). These KPs are done radially, the code search through the original CT KPs and gets the centroid from a *X*-*Y* dimension square over the ring. Axis *Z* values are standardized by using the new KPs medium value. Splines are made by a loop. This operation is fully automatic (Figure 6).

Manubrium, intermediate and central areas share the same algorithm with minor modification among them. This procedure is semi-automatic. A guide KP is created to search and make new KPs for the manubrium. These KPs are done by looking for the centroid in various areas along the path between the superior ring and the guide KP. The track is divided and new KPs are created between portions, using the centroid of those *X*-*Y* dimension areas. Splines are made (Figure 7A).

For the intermediate area the procedure is almost the same, but in this case the ends of the searching path are a KP from the superior ging or manubrium and another form the external perimeter. The same happens with the lines between the manubrium path, where a KP of each path is an end. At the central area, one end is a KP from the superior ring and the other is always the same, one point created at the centre of the TM (Figure 7B). All the lines are made using this new KPs and the search is finished.

Once all the lines are created, TM new areas are modeled (Figure 7C). These areas are extruded, and the TM geometry is finished as a volume. This part of the algorithm is not automatic due to the complexity of finding a numerical pattern for this procedure.

The remodeled TM is exported and saved using IGES format to be imported by ANSYS during the model building process.

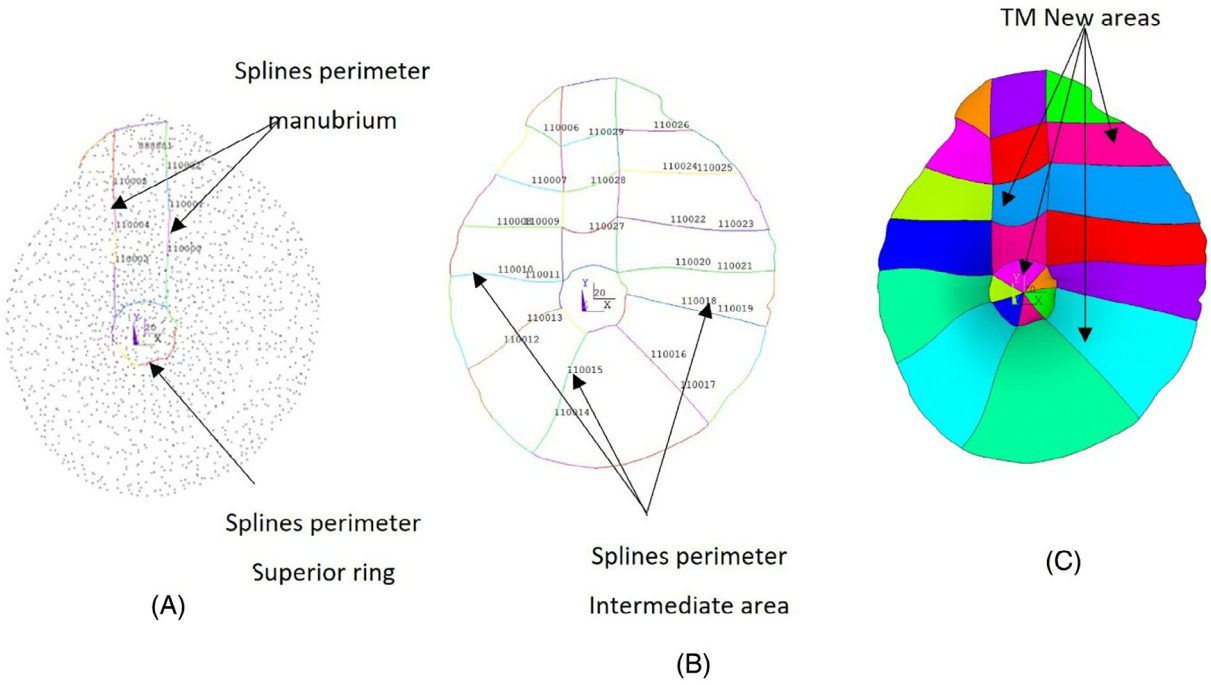

FIGURE 7 Data points, splines and areas of TM. (A) Manubrium and central perimeter with splines curves. (B) Manubrium, intermediate and central perimeter with splines curves. (C) TM new areas.

3.3 | Cavities and coupling

Once we have the new TM and the OC the next step is a coupling process, first among the TM and the OC through the MF connection and second among the whole system and the cavities.

The manubrium fold is a recently identified part of the hearing system[18] it is a material connecting the TM and the umbo. In our model, the MF is modeled by extruding known TM areas. These areas belong to the manubrium and central areas. The volume is redone after the extrusion and adapted to the approximate shape of the actual MF. The malleus contact zone is hollowed out and so the three components can be joint.

The coupling of the cavities implies the transformation of the part where they connect with the solid part of the model. The Micro-CT information does not include the EC, so we have used an EC geometry previously used[22,25] slightly scaled to adapt to the present specimen. The EC-TM coupling implies a total EC modification at its TM zone. Old lines and areas are deleted. New lines and areas are created using the final TM data as a guide. At this point, the OC, TM, and EC model is finished (Figure 8).

For the present work a simplified TC is created using[23] as a guide. It was made from sections shown in.[32] A primitive TC is made using KP from the modeled AS. This initial geometry is modified by hollowing out material. The TC geometry ends when the TM-TC coupling is made. The coupling is made by cutting a TM shaped hole and sealing it with TM data. This operation is semi-automatic, most of the job is done by referenced commands that need minor modifications (Figure 9).

Finally, at this point the model geometry is completed (Figure 10A). Now the next step is the meshing of the geometric component (Figure 10B) and the implementation of the boundary conditions.

Finite Element Model contain 208.710 elements: 27.564 solid 185; 181.109 Fluid30; 18 Shell181; 1 Combin14; and 19 Beam188.

From everything described above we can say that the algorithm is fully automated with regard to the construction of the volumes of the OC, tendons and suspensory ligaments. For TM, only the last step (extrusion of the areas) is manual.

The simplified models of the EC and TC are justified in this research because there are no STL files for them; However, the procedure used in the OC would be perfectly replicable if such files were available.

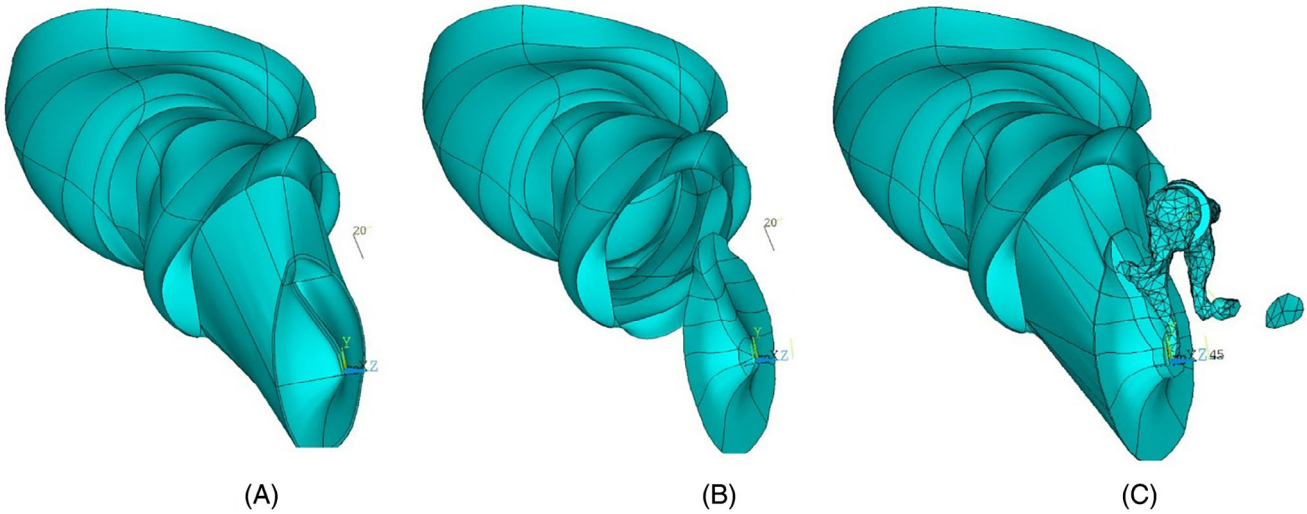

FIGURE 8 EC-TM coupling. (A) Original EC. (B) EC and new TM no coupling. (C) EC and middle ear coupling.

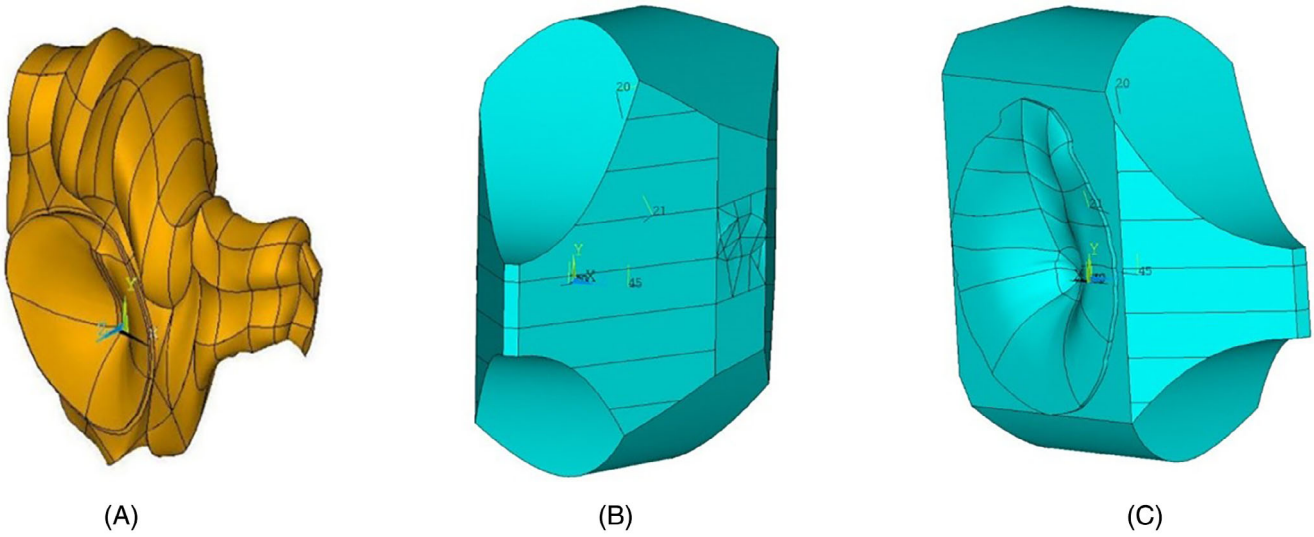

FIGURE 9 Modeling of TC. (A) TC guide. (B): Initial geometry TC. (C) TC geometry model finished.

Manual interventions in the algorithm are minor and are limited to adjusting the geometry of the borders between the MT and both cavities, in the coupling stage. With this algorithm it was possible to reduce the construction time of the model from 4 weeks to approximately 3 days.

3.4 | Numerical results

The main objective of this research is to demonstrate the viability of the application of the semi-automatic algorithm for the construction of a finite element model of the human hearing system, with a minimum investment of time and computing cost. This methodology can be used to build numerical models applied to patients.

To demonstrate the functionality and validation of the model generated in this research, a harmonic and modal analysis of the components of the middle ear is carried out, since there are numerical and experimental results that allow its validation.

A modal analysis of TM-OC coupling and TM (Figure 11 and Figure 12) was performed. Figure 12 shows the selected mode shapes. They follow a similar pattern compared with previous work.[29,33] For example, the classic

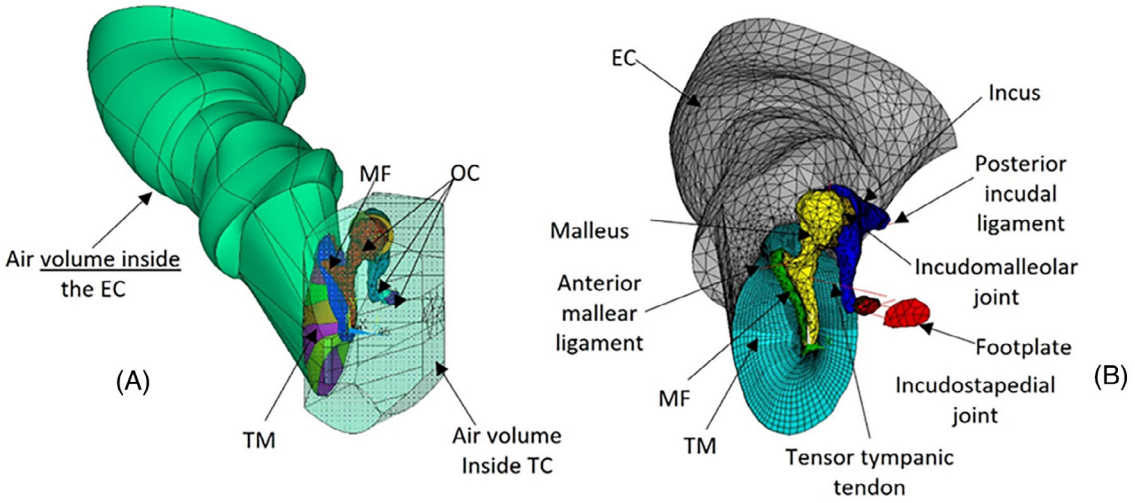

FIGURE 10 Geometric and Finite Element Model. (A) EC-TM-OC-CT geometric coupling. (B) Finite Element Model (TC not included).

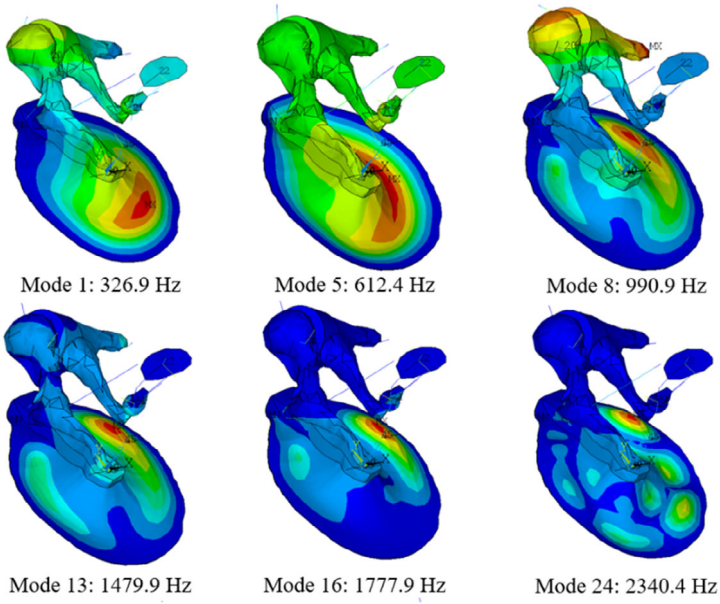

FIGURE 11 Selected mode shapes. TM-OC coupling.

piston-like motion of TM is observed in mode 5, which is equivalent to mode 1 in Figure 12. Mode 24 is equivalent to mode 6 of TM, which is a complex pattern.

Modes 8 and 13 (Figure 11) are representative of the starting point of the transition zone to ordered pattern. Finally, mode 50 (Figure 12) corresponds clearly to the ordered pattern, where a huge number of vibration modes can be observed with similar shapes.

These results are similar to those obtained by,[29] and follow a pattern close to those measured by.[33] Some differences in the values of the mode frequencies may be due to the geometric differences of the TM, since it is well known that TM greatly influences the dynamic response of the system.

Finally, a harmonic analysis was conducted from 100 to 10.000 Hz. A uniform harmonic 80 dB_{SPL} stimulus pressure was applied to the lateral side of the eardrum. The amplitude of umbo and stapes footplate displacements versus frequency is shown in Figure 13 compared with experimental measurements.[34]

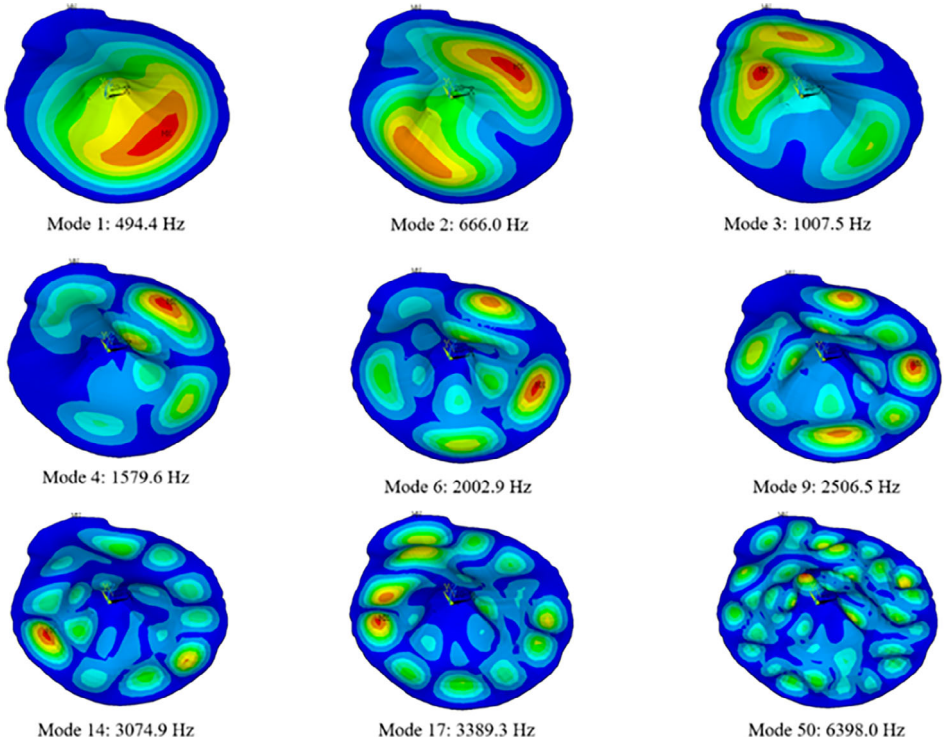

FIGURE 12 Selected mode shapes. TM Finite Element model.

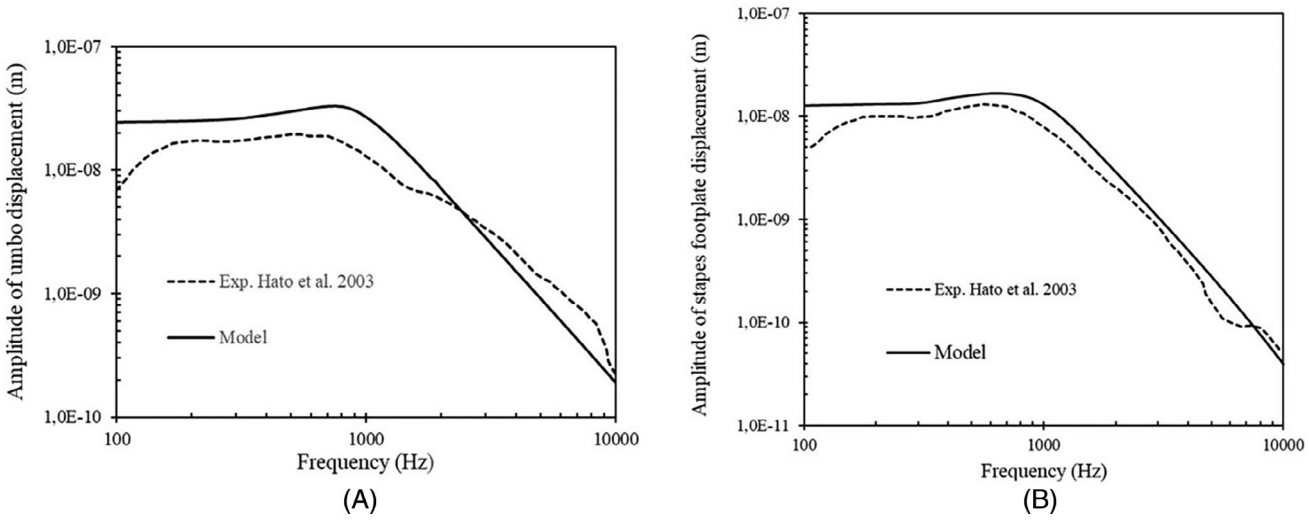

FIGURE 13 Amplitude of displacement versus frequency. (A) umbo. (B) stapes footplate. Range from 100 to 10.000 Hz at 80 dB_{SPL} sound pressure.

The behavior curves of the umbo and stapes are those expected and verified in the literature. A low frequency zone between 100 and 1000 Hz (maximum displacements) with a peak close to 900 Hz, then between 1000 and 3000 Hz defined as medium frequency and high frequency above 3000 Hz.

4 | CONCLUSION

This work is part of a line of research focused on the fully automated construction process of ear models of patients aimed at helping to identify and correct auditory pathologies through numerical simulations.

In this paper, a semi-automatic algorithm to build, from Micro-CT images, a numerical model of the human auditory system was described. Model parts are identified, simplified based on a post meshing strategy, properties are applied, and external boundary conditions and junctions are generated.

Despite not being fully automated, its implementation substantially reduces the construction time of model by approximately 90%, without generating meshing problems, in addition to low computational cost. Simulation results presented show accurate results respect previous models with same material properties.

On the other hand, this research allowed the application of structurally equivalent models, such as the stirrup case. In the future, ossicular chain components geometry could be simplified without significantly affecting their dynamic responses, easing their coupling through the described algorithm.

ACKNOWLEDGMENTS

The authors would like to thank the Universidad de Málaga/CBUA for their implication in this research.

FUNDING INFORMATION

This work has been funded by the Universidad de Málaga/CBUA and the European Regional Development Fund grant number UMA18-FEDERJA-214.

CONFLICT OF INTEREST STATEMENT

The authors declare that they have no competing interests.

DATA AVAILABILITY STATEMENT

The data that support the findings of this study are available from the corresponding author upon reasonable request.

ORCID

L. Caminos https://orcid.org/0000-0001-5695-8566

REFERENCES

1. Carretta R, Lorenzetti S, Müller R. Towards patient-specific material modeling of trabecular bone post-yield behavior. *Int J Numer Meth Biomed Eng*. 2013;29(2):250-272. doi:10.1002/cnm.2516
2. Vergari C, Ribes G, Aubert B, et al. Evaluation of a patient-specific finite-element model to simulate conservative treatment in adolescent idiopathic scoliosis. *Spine Deform*. 2015;3(1):4-11. doi:10.1016/j.jspd.2014.06.014
3. Courchesne O, Guibault F, Parent S, Cheriet F. Patient-specific anisotropic model of human trunk based on MR data. *Int J Numer Meth Biomed Eng*. 2015;31(9):1-18. doi:10.1002/cnm.2724
4. Hoermann JM, Pfaller MR, Avena L, Bertoglio C, Wall WA. Automatic mapping of atrial fiber orientations for patient-specific modeling of cardiac electromechanics using image registration. *Int J Numer Meth Biomed Eng*. 2019;35(6):e3190. doi:10.1002/cnm.3190
5. Wang D, Serracino-Inglott F, Feng J. Numerical simulations of patient-specific models with multiple plaques in human peripheral artery: a fluid-structure interaction analysis. *Biomech Model Mechanobiol*. 2021;20(1):255-265. doi:10.1007/s10237-020-01381-w
6. Koike T, Wada H, Kobayashi T. Modeling of the human middle ear using the finite-element method. *J Acoust Soc Am*. 2002;111(3):1306-1317. doi:10.1121/1.1451073
7. Gan RZ, Feng B, Sun Q. Three-dimensional finite element modeling of human ear for sound transmission. *Ann Biomed Eng*. 2004;32(6):847-859. doi:10.1023/B:ABME.0000030260.22737.53
8. Prendergast PJ, Ferris P, Rice HJ, Blayney AW. Vibro-acoustic modelling of the outer and middle ear using the finite-element method. *Audiol Neurotol*. 1999;4(3–4):185-191. doi:10.1159/000013839
9. Kelly DJ, Prendergast PJ, Blayney AW. The effect of prosthesis design on vibration of the reconstructed ossicular chain: a comparative finite element analysis of four prostheses. *Otol Neurotol*. 2003;24(1):11-19. doi:10.1097/00129492-200301000-00004
10. Wada H, Kobayashi T. Dynamical behavior of middle ear: theoretical study corresponding to measurement results obtained by a newly developed measuring apparatus. *J Acoust Soc Am*. 1990;87(1):237-245. doi:10.1121/1.399290
11. Sun Q, Gan RZ, Chang K-H, Dormer KJ. Computer-integrated finite element modeling of human middle ear. *Biomech Model Mechanobiol*. 2002;1(2):109-122. doi:10.1007/s10237-002-0014-z
12. Williams KR, Lesser THJ. A finite element analysis of the natural frequencies of vibration of the human tympanic membrane. *Part I. British J Audiol*. 1990;24(5):319-327. doi:10.3109/03005369009076572
13. De Greef D, Pires F, Dirckx JJJ. Effects of model definitions and parameter values in finite element modeling of human middle ear mechanics. *Hear Res*. 2017;344:195-206. doi:10.1016/j.heares.2016.11.011
14. Zhou L, Shen N, Feng M, Liu H, Duan M, Huang X. Morphology of human ear canal and its effect on sound transmission. *Int J Numer Meth Biomed Eng*. 2022;38(3):1-12. doi:10.1002/cnm.3567

15. Zhang J, Tian J, Ta N, Rao Z. Finite element analysis of round-window stimulation of the cochlea in patients with stapedial otosclerosis. *J Acoust Soc Am*. 2019;146(6):4122-4130. doi:10.1121/1.5134770
16. Decraemer WF, Dirckx JJJ, Funnell WRJ. Three-dimensional modelling of the middle-ear ossicular chain using a commercial high-resolution X-ray CT scanner. *J Assoc Res Otolaryngol*. 2003;4(2):250-263. doi:10.1007/s10162-002-3030-x
17. Sim JH, Puria S. Soft tissue morphometry of the malleus–incus complex from micro-CT imaging. *J Assoc Res Otolaryngol*. 2008;9(1):5-21. doi:10.1007/s10162-007-0103-x
18. De Greef D, Goyens J, Pintelon I, et al. On the connection between the tympanic membrane and the malleus. *Hear Res*. 2016;340:50-59. doi:10.1016/j.heares.2015.12.002
19. De Greef D, Buytaert JAN, Aerts JRM, Van Hoorebeke L, Dierick M, Dirckx J. Details of human middle ear morphology based on micro-CT imaging of phosphotungstic acid stained samples. *J Morphol*. 2015;276(9):1025-1046. doi:10.1002/jmor.20392
20. Tang H, Psota P, Rosowski JJ, Furlong C, Cheng JT. Analyses of the tympanic membrane impulse response measured with high-speed holography. *Hear Res*. 2021;410:108335. doi:10.1016/j.heares.2021.108335
21. Garcia-Manrique J, Furlong C, Gonzalez-Herrera A, Cheng JT. Numerical model characterization of the sound transmission mechanism in the tympanic membrane from a high-speed digital holographic experiment in transient regime. *Acta Biomater*. 2023;159:63-73. doi:10.1016/j.actbio.2023.01.048
22. Caminos L, Garcia-Gonzalez A. Gonzalez-Herrera a. numerical analysis of the influence of the auditory External Canal geometry on the human hearing response. *Proceedings of the 11th International Mechanics of Hearing Workshop*. AIP Publishing; 2011:515-520.
23. Garcia-Gonzalez A, Gonzalez-Herrera A. Effect of the middle ear cavity on the response of the human auditory system. *Proceeding of Meeting of Acousting*. AIP; 2013:30099.
24. Chaves G. *Complete Modeling of the Human Hearing System Including Cavities*. University of Malaga; 2022.
25. Caminos L. *Study of the Influence of Parameters in the Numerical Modeling of the Behavior of the Human Middle and External Ear*. University of Malaga; 2011.
26. De Greef D, Aernouts J, Aerts J, et al. Viscoelastic properties of the human tympanic membrane studied with stroboscopic holography and finite element modeling. *Hearing Research*. 2014;312:69-80. doi:10.1016/j.heares.2014.03.002
27. Weistenhöfer C, Hudde H. Determination of the shape and inertia properties of the human auditory ossicles. *Audiology and Neurotology*. 1999;4(3–4):192-196. doi:10.1159/000013840
28. Speirs AD, Hotz MA, Oxland TR, Häusler R, Nolte L-P. Biomechanical properties of sterilized human auditory ossicles. *Journal of Biomechanics*. 1999;32(5):485-491. doi:10.1016/s0021-9290(99)00012-3
29. Caminos L, Garcia-Manrique J, Lima-Rodriguez A, Gonzalez-Herrera A. Analysis of the mechanical properties of the human tympanic membrane and its influence on the dynamic behaviour of the human hearing system. *Applied Bionics and Biomechanics*. 2018;2018:1-12. doi:10.1155/2018/1736957
30. Volandri G, Di Puccio F, Forte P, Carmignani C. Biomechanics of the tympanic membrane. *Journal of Biomechanics*. 2011;44(7):1219-1236. doi:10.1016/j.jbiomech.2010.12.023
31. Cheng T, Gan RZ. Mechanical properties of stapedial tendon in human middle ear. *Journal of Biomechanical Engineering*. 2007;129(6):913-918. doi:10.1115/1.2800837
32. Gulya AJ. *Anatomy of the temporal bone with surgical implications*. CRC Press; 2007.
33. Rosowski JJ, Cheng JT, Ravicz ME, et al. Computer-assisted time-averaged holograms of the motion of the surface of the mammalian tympanic membrane with sound stimuli of 0.4–25kHz. *Hearing Research*. 2009;253(1–2):83-96. doi:10.1016/j.heares.2009.03.010
34. Hato N, Stenfelt S, Goode RL. Three-dimensional stapes footplate motion in human temporal bones. *Audiology and Neurotology*. 2003;8(3):140-152. doi:10.1159/000069475

How to cite this article: Caminos L, Chaves G, Garcia-Manrique J, Gonzalez-Herrera A. Semi-automatic algorithm to build finite element numerical models of the human hearing system from Micro-CT data. *Int J Numer Meth Biomed Engng*. 2024;e3817. doi:10.1002/cnm.3817